Inclusive K_S^0, Λ, and $\bar{\Lambda}$ production in $\pi^+ d$ interactions at 24 GeV/c

S. Dado, J. Goldberg, and S. Toaff
Department of Physics, Technion—Israel Institute of Technology, Haifa, Israel

A. Av-Shalom and J. Grunhaus
Department of Physics and Astronomy, Tel-Aviv University, Ramat Aviv, Israel

(Received 7 February 1980)

We have studied inclusive K_S^0, Λ, and $\bar{\Lambda}$ production in $\pi^+ d$ interactions at 24 GeV/c. The observed cross sections are 2.5 ± 0.13 mb for K_S^0, 1.62 ± 0.09 mb for Λ, and 0.12 ± 0.02 mb for $\bar{\Lambda}$. Longitudinal- and transverse-momentum distributions of the produced particles are presented. The average charged multiplicities of the system associated with a K_S^0 or with a Λ are presented and discussed. A nonzero average Λ polarization (-0.10 ± 0.03) is observed. The x distribution of the backward (forward) K_S^0 and Λ produced in the reaction are in agreement with the x distribution of valence quarks in nucleons in nuclear target (pion beam), as predicted by the quark-recombination model of particle production applied to nuclear targets.

INTRODUCTION

Extensive data on inclusive strange-particle production are available in the literature from interactions of pion and proton beams on a proton target.[1-8] Data on strange-particle production from a deuteron target are scarce. The deuteron, as the simplest nucleus, may provide a simple case to examine models of particle production applied to nuclear targets. Such an attempt was made by Berlad, Dar, and Eilam[9] where they applied the quark-recombination model to nuclear targets using a quark-parton picture of nuclei in a high-momentum frame. In their model, the hadron-nucleus collision is viewed as a collision with the nucleons lying within a cylinder (tube) of specified cross section along the path of the beam particle through the nucleus. In the case of an interaction with a deuteron nucleus, the tube will contain either one or two nucleons.

In this paper we present experimental data on strange-particle production from deuteron targets and analyze it within a quark-recombination model applied to nuclear targets as outlined above.[9]

The following inclusive reactions have been studied:

$$\pi^+ d \to K_S^0 + X\,, \tag{1}$$

$$\pi^+ d \to \Lambda + X\,, \tag{2}$$

$$\pi^+ d \to \bar{\Lambda} + X\,. \tag{3}$$

The experimental procedure is described in Sec. II. Total and topological cross sections are given in Sec. III. In Sec. IV we present inclusive distributions of the center-of-mass production angle θ^*, Feynman x, rapidity, transverse momentum p_T, and average charge multiplicity $\langle n_X \rangle$ of the system of particles produced with the K_S^0, Λ, and $\bar{\Lambda}$. In Sec. V the polarization of the Λ particles is presented. The analysis of the data is presented in Sec. VI, and a summary of the results and conclusions are given in Sec. VII.

II. EXPERIMENTAL PROCEDURE

The data for this study are taken from an exposure of the 80-in. bubble chamber at Brookhaven National Laboratory filled with deuterium to a 24-GeV/c π^+ beam. About 83 000 pictures were scanned for a visible V^0 originating from a $\pi^+ d$ interaction vertex. Part of the film was double scanned in order to determine the scanning efficiency for the different topological final states.

The analysis which is presented here is based on about 8750 $\pi^+ d$ interactions leading to final states having one or more visible V^0's or γ-like events. These events were measured on hand digitizing machines, and the data were processed through the TVGP-SQUAW chain of programs. The following decay and γ-conversion hypotheses were attempted:

$$K_S^0 \to \pi^+ \pi^-\,, \tag{4}$$

$$\Lambda \to p \pi^-\,, \tag{5}$$

$$\bar{\Lambda} \to \bar{p} \pi^+\,, \tag{6}$$

$$\gamma d \to e^+ e^- d\,. \tag{7}$$

The following procedure was used in the process of separation between competing hypotheses.

Only three-constraint (3C) fits, in which the neutral particle was required to come from the primary vertex of the interaction, were accepted. V^0's uniquely fitting hypothesis (7) were removed from the sample. To eliminate further electron-pair contamination in the data, the decay tracks of all remaining V^0's were tentatively assumed to be electrons, and the distribution of the unfitted invariant mass of the possibly fake electron

pairs was examined. An enhancement of events around $M(e^+e^-)=0$ was observed which tapered off sharply after $M(e^+e^-)=45$ MeV. Thus all events with $M(e^+e^-)\leq 45$ MeV were rejected from the sample. We discarded from the remaining sample the events with γ/K_S^0 ambiguity, because their $M(e^+e^-)$ is found to be much lower than that expected for genuine K_S^0 events. Events with γ/Λ or $\gamma/\bar{\Lambda}$ ambiguity were removed from the remaining sample only if the confidence level (C.L.) of the γ fit was higher than the C.L. of the Λ or the $\bar{\Lambda}$ fit. This was done because low $M(e^+e^-)$ values down to 45 MeV may still be obtained for genuine Λ and $\bar{\Lambda}$ events because of the low Q value of their decays. After applying a fiducial volume cut for the primary vertex and the V vertex and a cut of 0.8 cm on the minimum flight distance between these vertices, and after removing fits with $\chi^2>18$, a sample of 2633 events was left. This sample contains 2774 neutral strange particles each of which fits one or more of hypotheses (4)–(6). About 19% of these V's have more than one fit. The distribution of the fits is shown in Table I.

To resolve the Λ/K_S^0 ambiguous events, we plot for the unambiguous K_S^0 fits the unfitted invariant mass of their decay products with (p,π^-) mass assignment [unshaded area of Fig. 1(a)]. The missing events at the Λ mass should come from a correct assignment of events with K_S^0/Λ ambiguity since by definition such events fit Λ hypothesis.

Similarly, one finds a dip at the K_S^0 mass in the fake $M(\pi^+\pi^-)$ plot of the decay products of unambiguous Λ fits [unshaded area of Fig. 1(b)]. Again these missing events fit by definition the K_S^0 hypothesis, and a correct assignment of Λ/K_S^0 ambiguous events should fill in the dip. A similar effect (not shown) occurs when the few

TABLE I. Number of inclusive V^0 particles after a 3C kinematical fit and cuts on M^2, χ^2, fiducial volume, and flight distance (see text).

	Events	Weighted events[a]	Average weight[a]
Unique K_S^0	1461	1639	1.122
Unique Λ	739	825	1.116
Unique $\bar{\Lambda}$	39	44	1.133
Ambiguous K_S^0/Λ	426		
Ambiguous $K_S^0/\bar{\Lambda}$	108		
Ambiguous $\Lambda/\bar{\Lambda}$	1		
Resolved K_S^0	1620	1820	1.123
Resolved Λ	1082	1226	1.133
Resolved $\bar{\Lambda}$	72	83	1.150

[a] For escape probability.

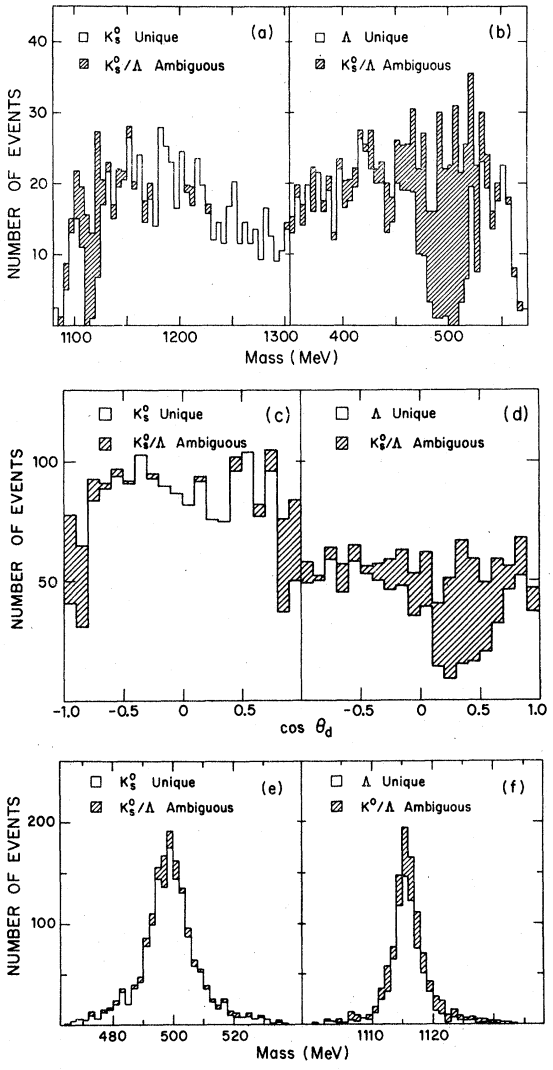

FIG. 1. (a), (b), (e), (f) Effective-mass distributions of V^0 decay products with fake [(a), (b)] and correct [(e), (f)] mass assignments as described in the text. (c), (d) Distributions of $\cos\theta_d$ (where θ_d is the angle between the positive decay product and the incoming V^0 direction in the V^0 rest frame) for K_S^0 and Λ events, respectively. The unshaded area denotes unambiguous events, and the shaded area denotes ambiguous events resolved by the method described in the text.

unique $\bar{\Lambda}$ events are plotted as $M(\pi^+\pi^-)$ and when unique K_S^0 events are plotted as $M(\bar{p}\pi^+)$.

To find a proper assignment for the ambiguous fits, we tried different cuts based on C.L. comparison and chose those cuts which filled in properly the dips observed in figures like 1(a) and 1(b). We find the following criteria as satisfactory: for K_S^0/Λ ambiguities, the fit was accepted as Λ if

$$1.5\times \text{C.L.}(\Lambda) > \text{C.L.}(K_S^0);$$

for $K_S^0/\bar{\Lambda}$ ambiguities, the fit was accepted as K_S^0 if

$$2\times \text{C.L.}(K_S^0) > \text{C.L.}(\bar{\Lambda}).$$

The K^0/Λ ambiguous events separated by these criteria are shown in the shaded parts of Figs. 1(a) and 1(b). To check the method used to resolve the ambiguities we plot in Figs. 1(c) and 1(d) the decay angle θ_d, the angle between the positive decay product, and the incoming V^0 direction in the V^0 rest frame. The resolved ambiguous events (shaded areas) bring the final plots to a form which is consistent with isotropy, as expected.

As a further check to the method, one expects from the symmetry of K_S^0 decay the number of K_S^0 events resolved from the K^0/Λ ambiguous sample to be equal within statistics to the number of K_S^0 events from the $K_S^0/\bar{\Lambda}$ ambiguous sample. We find this check also satisfactory in our data: 84 K_S^0 events were resolved out of 426 K_S^0/Λ ambiguous events and 75 K_S^0 events were resolved out of 108 $K_S^0/\bar{\Lambda}$ ambiguous events. The invariant unfitted mass distributions for the unique and for the total resolved sample are shown in Figs. 1(e) and 1(f) for the K_S^0 and Λ, respectively. The K_S^0 and Λ samples have mass averages of 498.8 ± 0.3 and 1116.0 ± 0.1 MeV with apparent widths of 10 and 4 MeV, respectively, which indicate fair experimental resolution. Final numbers of fits are presented in Table I. Each V^0 was weighted to correct for those events which escaped the chamber before decaying or decayed within 0.8 cm of the primary vertex. The usual weighting procedure was followed. The mean decay paths were determined from the known lifetimes. The number of events weighted by escape probability and the average weight are given in Table I. In the rest of the paper the term "weighted event" always refers to weighting by this escape probability only.

III. TOTAL AND TOPOLOGICAL CROSS SECTIONS

The cross sections for the various channels were determined as a function of topology. Corrections have been made for detection, measuring, and fitting losses as well as for the neutral decay modes of the strange particles. However, no correction was made for the contamination from K_L nor for the unavoidable inclusion of Σ^0 events. The topological and total cross sections are given in Table II in which odd-prong events were increased by one to account for the unseen proton spectator. The quoted errors include estimates of uncertainty in each of the corrections made in addition to the statistical error.

One observes from Table II that all topological cross sections for reactions (1)–(3) peak at four prongs while the average charge multiplicity is similar for K_S^0 and Λ production (4.93 ± 0.04 and 4.95 ± 0.05, respectively) but is slightly lower (4.69 ± 0.18) for $\bar{\Lambda}$ production. The three samples have also the same dispersion

$$D = (\langle n_{\text{ch}}^2\rangle - \langle n_{\text{ch}}\rangle^2)^{1/2}$$

within errors. Moreover, the cross sections for K_S^0 inclusive production are roughly 1.5 times larger than that for Λ production (total cross sections as well as topological). However, the cross sections for $\bar{\Lambda}$ inclusive production, which involves baryon-antibaryon production, are more than one order of magnitude lower than those of the K_S^0 and Λ production.

IV. INCLUSIVE DISTRIBUTIONS

A. Center-of-mass production angle θ^*

In this paper, unless otherwise stated, by "center-of-mass" system, we refer to the system of the projectile and a single nucleon target in the deuteron assumed to be at rest.

TABLE II. Neutral-strange-particles inclusive cross sections for $\pi^+ d \to K_S^0 + X$, $\Lambda + X$, and $\bar{\Lambda} + X$. n_{ch} is increased by one for odd-prong events to account for the unseen proton spectator. The cross sections are corrected for neutral decay modes.

n_{ch} (number of charged prongs)	$\sigma(\mu b)$ K_S^0	Λ	$\bar{\Lambda}$
2	375 ± 44	224 ± 31	21 ± 6
4	1023 ± 97	692 ± 70	52 ± 12
6	739 ± 73	474 ± 49	29 ± 9
8	294 ± 35	181 ± 25	11 ± 4
10	62 ± 13	47 ± 12	4 ± 3
12	6 ± 3	4 ± 3	
Total inclusive	2.50 ± 0.13 mb	1.62 ± 0.09 mb	0.12 ± 0.02 mb
$\langle n_{\text{ch}}\rangle$	4.93 ± 0.04	4.95 ± 0.05	4.69 ± 0.18
$D = (\langle n_{\text{ch}}^2\rangle - \langle n_{\text{ch}}\rangle^2)^{1/2}$	1.96 ± 0.03	1.95 ± 0.04	1.96 ± 0.13

Figure 2 shows the number of weighted events for reactions (1)–(3) as a function of the K^0_S, Λ, and $\bar{\Lambda}$ center-of-mass production angle θ^*. In the K^0_S and the $\bar{\Lambda}$ distributions about 65% of the events are produced in the forward hemisphere. The Λ distribution exhibits a strong backward peak indicating that the Λ's are produced mainly in the target region. Similar features were observed in $\pi^+ p$ interactions at 16 GeV/c[1] and at 18.5 GeV/c.[2]

In Table III we give the asymmetry parameter $A = (F-B)/(F+B)$, where F and B denote the weighted number of events produced in the forward and backward hemispheres, respectively. The asymmetry in K^0_S production decreases from 0.44 to 0 (within error) as the number of charged prongs increases from 2 to 12 and averages at 0.28 ± 0.02. However, the Λ production seems to have an asymmetry which does not vary much with multiplicity and averages at -0.51 ± 0.02, a much higher value in magnitude than the average for the K^0_S production. Likewise, the $\bar{\Lambda}$ production seems to have an asymmetry which is not varying with multiplicity, as in the Λ case and is consistent with being a constant equal to the overall average of A: 0.36 ± 0.10, a value which is a little higher than the average for the K^0_S production.

TABLE III. Asymmetry parameter $A = (F-B)/(F+B)$. n_{ch} is increased by 1 for odd-prong events to account for the unseen proton spectator.

n_{ch} (Number of charged prongs)	K^0_S	Λ	$\bar{\Lambda}$
2	0.44 ± 0.05	-0.49 ± 0.07	0.30 ± 0.25
4	0.28 ± 0.04	-0.57 ± 0.04	0.43 ± 0.15
6	0.27 ± 0.04	-0.50 ± 0.05	0.16 ± 0.22
8	0.22 ± 0.07	-0.35 ± 0.08	0.45 ± 0.33
10	-0.10 ± 0.15	-0.46 ± 0.15	
12	-0.01 ± 0.48		
All topologies	0.28 ± 0.02	-0.51 ± 0.03	0.36 ± 0.10

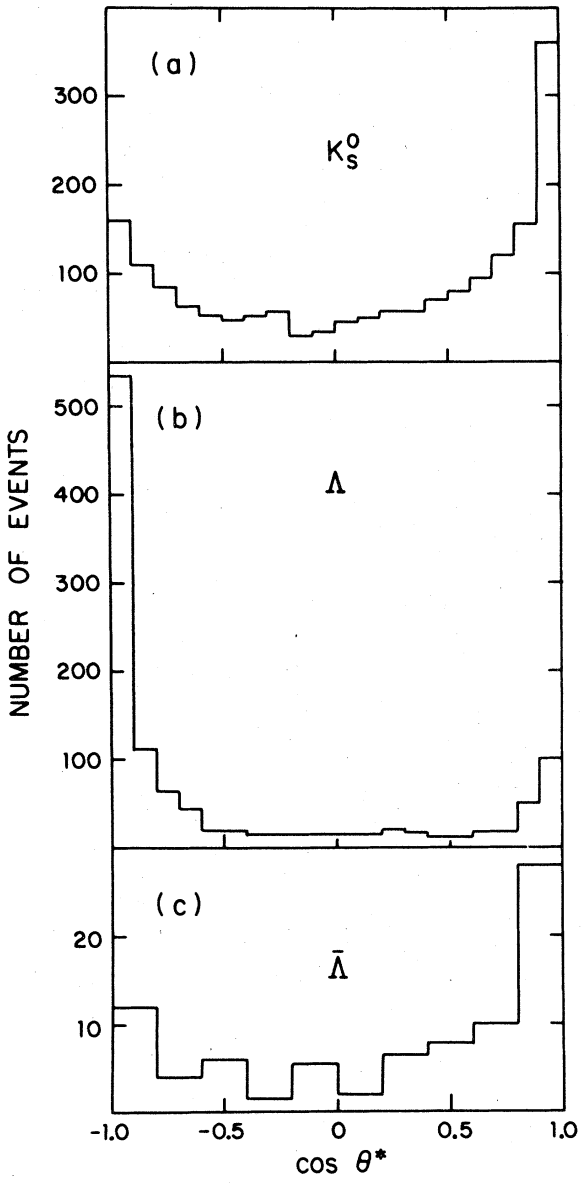

FIG. 2. Distributions of the cosine of the center-of-mass production angle θ^* for the (a) K^0_S's, (b) Λ's, and (c) $\bar{\Lambda}$'s.

Our production asymmetries for K^0_S, Λ, and $\bar{\Lambda}$ (0.28 ± 0.02, -0.51 ± 0.025, and 0.36 ± 0.03, respectively) are in good agreement with those (0.32 ± 0.02, -0.56 ± 0.02, and 0.36 ± 0.09) reported in a $\pi^+ p$ experiment[1] at 16 GeV/c. This is expected assuming that the same production mechanism is responsible for K^0_S, Λ, and $\bar{\Lambda}$ production in both $\pi^+ p$ and $\pi^+ d$ interactions.

B. Longitudinal variables

In Fig. 3 we show the invariant cross section

$$F(x) = \frac{1}{\pi p^*_{max}} \int E^* \frac{d^2\sigma}{dx\, dp_T{}^2}\, dp_T{}^2$$

for inclusive K^0_S, Λ, and $\bar{\Lambda}$ production, where $x = p_l^*/p^*_{max}$, and E^*, p_l^*, and p^*_{max} are the energy, the longitudinal momentum, and the maximum momentum (allowed by kinematics) of the produced V^0 in the overall center-of-mass system of the projectile, and a nucleon target assumed to be at rest in the deuteron. The $F(x)$ distribution for K^0_S production is shifted towards positive x while the distribution for Λ is shifted towards negative x. The distributions for K^0_S and for Λ peak at $x \cong 0.1$ and $x \cong -0.5$, respectively. These features have also been observed in $\pi^\pm p$ and pp experiments at similar and at much higher energies.[1-5] In Fig. 4 we show the center-of-mass

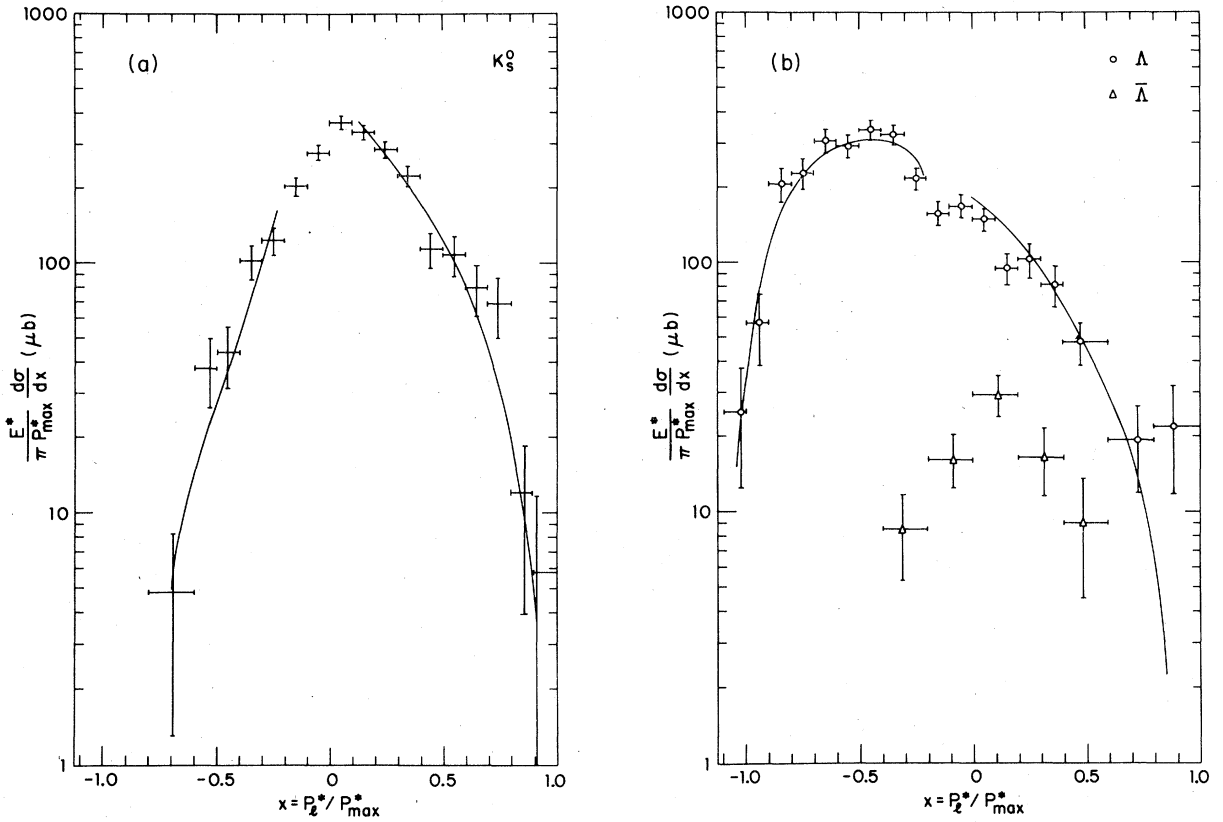

FIG. 3. Distributions of $(E^*/\pi p^*_{max})(d\sigma/dx)$ as a function of x for inclusive (a) K^0_S, and (b) Λ and $\bar{\Lambda}$ production. The solid lines are fits to the data as described in the text.

rapidity distributions $(1/\pi)d\sigma/dy^*$, where

$$y^* = \tfrac{1}{2} \ln \frac{E^* + p_l^*}{E^* - p_l^*} .$$

These distributions contain essentially the same information as the $F(x)$ distributions.

C. Transverse momentum p_T

The transverse-momentum-squared distributions $d\sigma/dp_T{}^2$ for K^0_S, Λ, and $\bar{\Lambda}$ production are shown in Fig. 5. We fitted to the data for small $p_T{}^2$ the functional form $ae^{-bp_T{}^2}$. The results of the fits are shown as solid lines in the figure. The values of a and b for K^0_S, Λ, and $\bar{\Lambda}$ production are given in Table IV.

Our results for the slopes b in Λ and in $\bar{\Lambda}$ production are compatible with results from other experiments at nearby and higher energies with p and π^- beams (21–28 GeV/c,[6] 205 GeV/c,[7] 250 GeV/c,[8] and 405 GeV/c[5]).

At high $p_T{}^2$ ($p_T{}^2 > 0.6$) the K^0_S slope drops and follows closely the Λ distribution both in shape and in absolute value. This feature has also been observed in the $\pi^+ p$ interaction at 16 GeV/c,[1] in the $\pi^- p$ interaction at 15 GeV/c,[3] and in the pp interaction at 405 GeV/c.[5]

The common slope at high $p_T{}^2$ (see Table IV) may come from a common mechanism in which particles are directly produced.[10] In this model the steeper slopes observed at small $p_T{}^2$ for lighter particles (pions and kaons) are produced by the addition of resonance decay products.

The average transverse momentum for each of the three processes considered is consistent with being constant as a function of charge multiplicity. The p_T averages over all multiplicities are

$$\langle p_T \rangle_{K^0_S} = 447 \pm 6 \text{ MeV}/c ,$$

$$\langle p_T \rangle_{\Lambda} = 507 \pm 8 \text{ MeV}/c ,$$

$$\langle p_T \rangle_{\bar{\Lambda}} = 538 \pm 28 \text{ MeV}/c .$$

We note that the $\langle p_T \rangle$ values for Λ and $\bar{\Lambda}$ are equal to each other, within errors, and it appears that $\langle p_T \rangle$ increases with mass of the produced particle.[2] Finally we show in Fig. 6 $\langle p_T{}^2 \rangle$ as a function of the Feynman variable x. The curves in the figure are a rough hand drawing to guide the eye. A strong x dependence of $P_T{}^2$ is evident in all three cases. This implies that the invariant cross

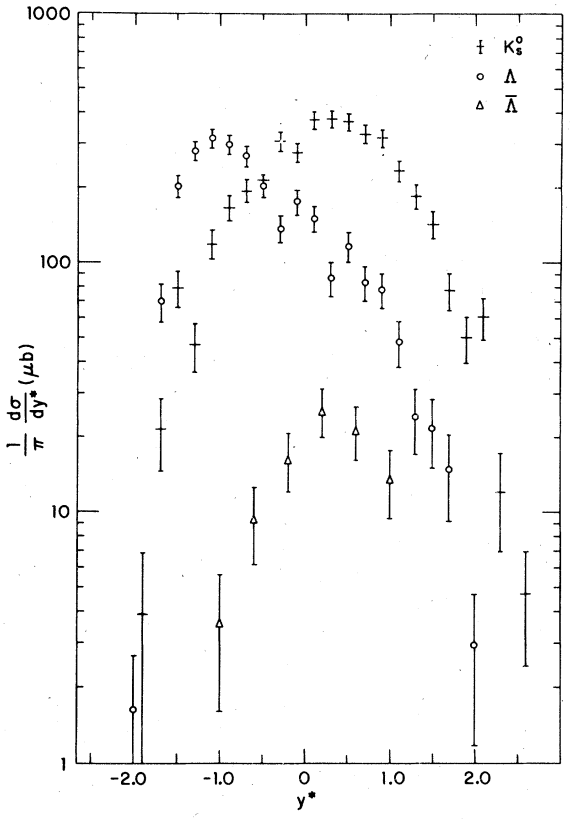

FIG. 4. Center-of-mass rapidity distributions $(1/\pi)$ $(d\sigma/dy^*)$ as a function of y^* for inclusive K_S^0, Λ, and $\bar{\Lambda}$ production.

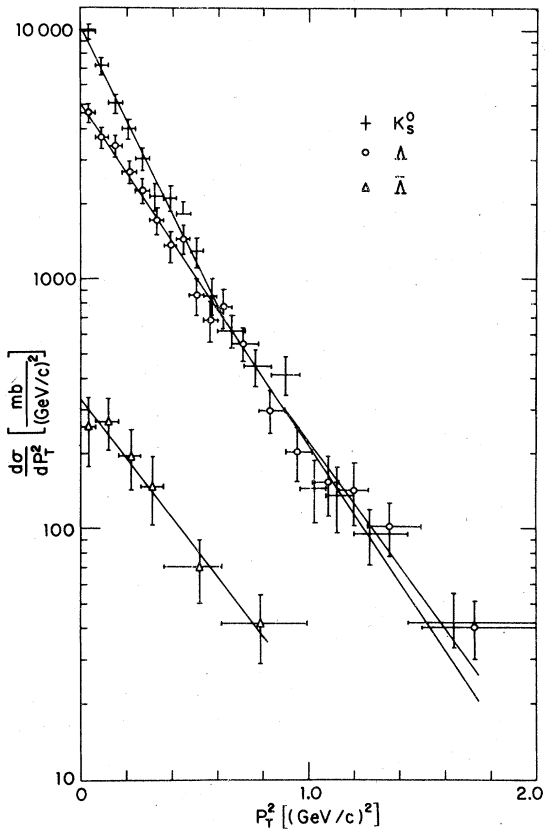

FIG. 5. Distributions of $d\sigma/dp_T{}^2$ as a function of $p_T{}^2$ for inclusive K_S^0, Λ, and $\bar{\Lambda}$. The solid lines represent fits to the function $ae^{-bp_T{}^2}$. (See Table IV for values of the parameters a and b.)

section

$$F(x,p_T{}^2)=\frac{E^*}{\pi p^*_{\max}}\frac{d^2\sigma}{dx\,dp_T{}^2}$$

does not factorize with respect to x and $p_T{}^2$. It is possible that this lack of factorization is due to the relatively low energy of our experiment. It will be of great interest to know whether factorization with respect to x and $p_T{}^2$ exists at higher energies.

Figure 6 also indicates that $\langle p_T{}^2\rangle$ for K_S^0 production in the beam (target) fragmentation region is similar in shape to $\langle p_T{}^2\rangle$ for Λ production in the target (beam) fragmentation region. In the central region, the shape of $\langle p_T{}^2\rangle$ for all three particles is consistent with U shape.

D. Average charged multiplicities $\langle n_x\rangle$

The average charged multiplicities $\langle n_X\rangle$ of the system of particles produced with the K_S^0 and with the Λ are plotted in Fig. 7(a) as a function of $M_X{}^2$ (the square of the invariant mass) recoiling against the V^0. In Fig. 7(b) only K_S^0 produced with $\cos\theta^*>0.5$ (48% of the sample) and Λ produced with $\cos\theta^*<-0.5$ (68% of the sample) are included. This was done in order to select those events in

TABLE IV. Parameters for the fits $d\sigma/dp_T{}^2=ae^{-bp_T{}^2}$.

Reaction	Range of $p_T{}^2$ for fit $[(GeV/c)^2]$	a [mb/(GeV/c)^2]	b $[(GeV/c)^{-2}]$	χ^2/DF
$\pi^+ d\to K_S^0+X$	0–0.6	10.26±0.46	4.30±0.10	9.2/8
	0.6–2.0	4.12±0.12	2.91±0.12	6.0/5
$\to\Lambda+X$	0–2.0	4.99±0.23	3.14±0.29	13.7/16
$\to\bar{\Lambda}+X$	0–1.0	0.33±0.06	2.70±0.48	0.9/4

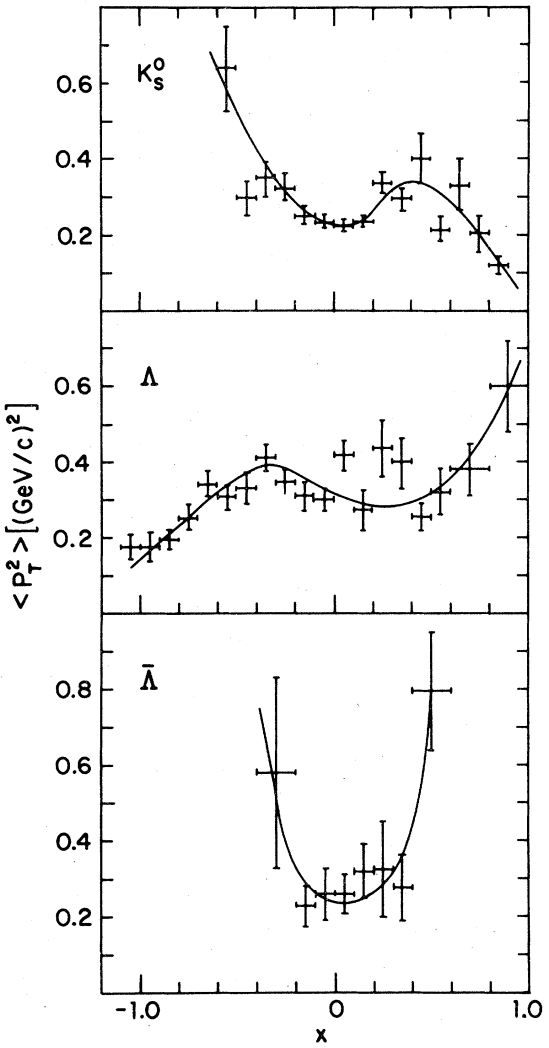

FIG. 6. Values of the average transverse momentum squared $\langle p_T^2 \rangle$ as a function of x for inclusive K_S^0, Λ, and $\bar{\Lambda}$ production. The curves are a rough hand drawing to guide the eye.

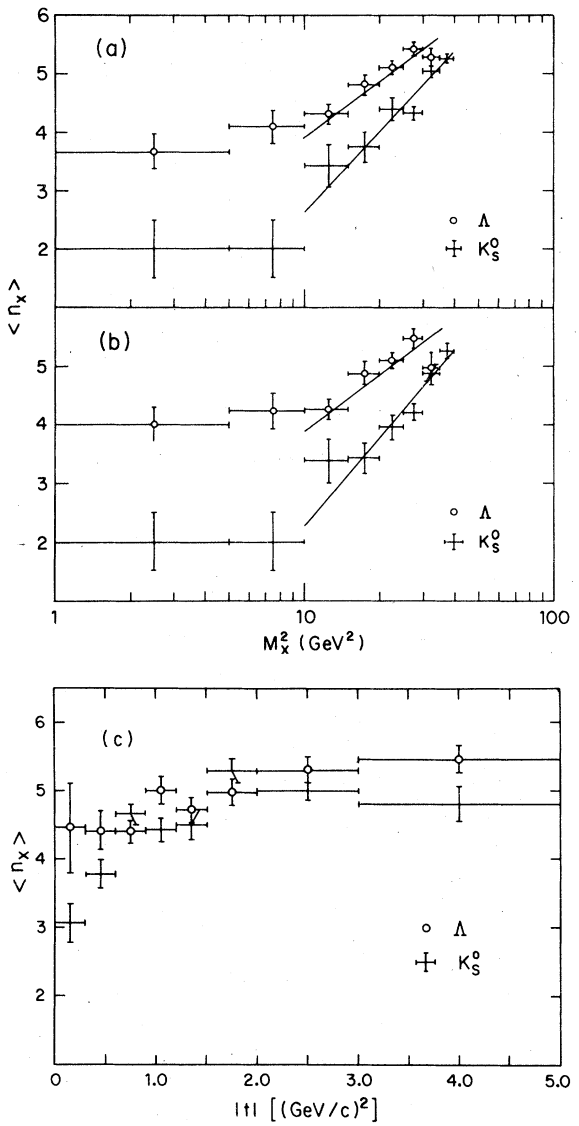

FIG. 7. (a) Average charged multiplicity $\langle n_X \rangle$ as a function of M_X^2 (see text) for inclusive K_S^0 and Λ production. (b) Events from (a) with $\cos\theta^* > 0.5$ for K_S^0 production and with $\cos\theta^* < -0.5$ for Λ production. (c) $\langle n_X \rangle$ as a function of the four-momentum transfer t_{π^+,K_S^0} for K_S^0 production and $t_{N,\Lambda}$ for Λ production for those events in (b) with $M_X^2 > 10$ GeV^2. Solid lines are fits of the function $A + B \ln M_X^2$ to the data. (See text for values of the parameter B.)

which the K_S^0 is associated with the beam and the Λ is associated with the target. We fitted to the data for $M_X^2 > 10$ GeV^2 the form

$$\langle n_X \rangle = A + B \ln M_X^2$$

and obtained for the whole sample $B_\Lambda = 1.17 \pm 0.21$ and $B_{K_S^0} = 1.98 \pm 0.22$. The χ^2/DF of the fits are 3.67/3 and 9.7/4, respectively. When limiting $\cos\theta^*$ as above we correspondingly obtained $B_\Lambda = 1.20 \pm 0.25$ and $B_{K_S^0} = 2.20 \pm 0.26$, with χ^2/DF = 5.8/4 and 7.1/4.

The results of the fits are shown in the figures. We note that for each of the Λ and the K_S^0 samples there is no significant difference between Figs. 7(a) and 7(b). This feature is well expressed by the approximately equal values of the slopes obtained in the fits for the Λ and the K_S^0 samples.

We note, however, that the slopes B_Λ and $B_{K_S^0}$ are significantly different. This result disagrees with the predictions of some theoretical diffractive and multiperipheral models[11] according to which B should be independent of the nature of the particles involved in the reaction.

In Fig. 7(c) we show the dependence of $\langle n_X \rangle$ on

the four-momentum transfer t from the beam (target) to the produced K_S^0 (Λ). [Figure 7(c) includes only those events from Fig. 7(b) with $M_X{}^2 > 10$ GeV^2.] One observes from Fig. 7(c) that the distributions for Λ and K_S^0 are similar within errors both in shape and in magnitude.

V. Λ POLARIZATION

The polarization P of the Λ's produced in our experiment in the target fragmentation region [defined by $x(\Lambda) \leq -0.2$] is shown in Fig. 8 as a function of x and of p_T. We used the relation

$$P = \frac{3}{\alpha} \langle \cos\theta_p \rangle ,$$

where the polarization angle θ_P is, as usual, defined by

$$\cos\theta_p = \frac{(\vec{\Lambda} \times \vec{\pi}) \cdot \vec{p}}{|\vec{\Lambda} \times \vec{\pi}|\,|\vec{p}|} .$$

$\vec{\pi}$ and $\vec{\Lambda}$ are the momenta of the incident π^+ and the produced Λ, respectively. $\vec{p}$ is the momentum of the decay proton in the Λ rest frame. α is the Λ-decay asymmetry parameter taken as 0.642.[12]

The error on P was calculated from the relation[13]

$$\Delta P = \tfrac{1}{2}\left[\frac{3 - (\alpha P)^2}{N}\right]^{1/2} ,$$

where N is the weighted number of observed Λ's.

In Fig. 8 one observes a negative polarization at high p_T values, the magnitude of which seems to increase with p_T.

As a function of x, the polarization exhibits a clearer structure. Vanishing at the value of x for which the invariant cross section becomes a maximum ($x \cong -0.6$, see Fig. 3), it reaches symmetrical extrema with respect to this point and then seems to decrease back to zero. The average polarization for $x < -0.2$ is $P = -0.10 \pm 0.03$.

The features of continuous increase of the Λ polarization with p_T for high p_T values and the nonzero average value of the polarization observed in our experiment have also been observed in a recent CERN ISR experiment at $\sqrt{s} = 53$ GeV.[14]

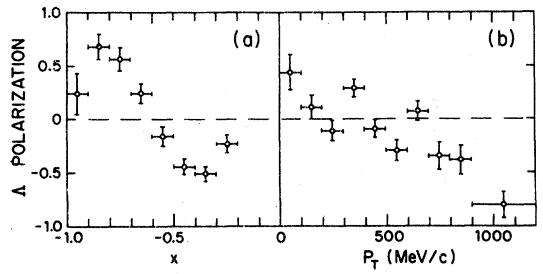

FIG. 8. Polarization of Λ as a function of (a) x, the Feynman variable, and (b) p_T, the transverse momentum, for the events with $x(\Lambda) \leq -0.2$.

VI. ANALYSIS OF x SPECTRA OF K_S^0 AND Λ PRODUCTION

In this section we study the Feynman-x dependence of the data and compare it with the prediction of the quark-recombination model.

The quark-recombination model is based on the observation by Ochs[15] that in the fragmentation region of a proton, the momentum distribution of a fast $\pi^+/(\pi^-)$ is similar to that of u (d) valence quark in the proton, as extracted from deep-inelastic electron-nucleon scattering experiments.[16,17] The parton-model mechanism proposed by Das and Hwa[18] to explain this observation assumed that meson production at large x results from the recombination of a fast valence quark q_v in the incident particle, which retains its original fractional momentum x, with a slow sea antiquark q_s ($x \sim 0$). The antiquark could either come from the original sea of the beam or of the target, or be excited by a gluon. Assuming that the recombination probability is independent of x, one expects that the x distribution of the produced meson will be similar to that of the quark in the projectile, in good agreement with experiment.[19]

The x distribution of the u quark and the d quark in a fast proton or neutron are well represented[20] by

$$u_p(x) = d_n(x) = \frac{35}{16}\,\frac{(1-x)^3}{\sqrt{x}} \tag{8}$$

and

$$d_p(x) = u_n(x) = \frac{315}{256}\,\frac{(1-x)^4}{\sqrt{x}} . \tag{9}$$

However, the x distribution of a valence quark in a fast pion is less certain. An approximate $(1-x)^2$ behavior was proposed by Ezawa[21] and by Berger and Brodsky.[22]

This prediction has been tested recently in experimental studies[23] of $\pi N \to \mu\bar{\mu}X$ and is consistent with the data.

We test here the idea of the recombination model for K_S^0 and Λ production in our experiment. We analyze separately the forward and the backward K_S^0 and Λ production.

A. Forward production of K_S^0

The incident π^+ ($u\bar{d}$) in our experiment and the $\bar{K}^0$ ($\bar{d}s$) component of the observed K_S^0 both contain a $\bar{d}$ quark. Hence, according to the recombination model, the K_S^0 production in the π^+

fragmentation region is the result of the recombination of the fast valence $\bar{d}$ quark in the projectile with a slow, strange (s) sea quark. Accordingly, one expects the x distribution of the produced K_S^0 to resemble the x distribution of the $\bar{d}$ quark in the projectile.

We have fitted to our data the predicted form $(1-x)^2$ and found a satisfactory result with $\chi^2/\mathrm{DF} = 10.9/7$ in the range $x(K_S^0) > 0.2$.[24] The result of the fit is shown as a curve in Fig. 3(a).

B. Forward production of Λ

Here the projectile π^+ and the produced Λ (uds) have in common a u quark. Therefore the Λ production in the projectile fragmentation region is the result of a recombination of the fast u quark in the projectile with a slow diquark (ds) from the sea. Again we have fitted to our data for forward Λ production the form $(1-x)^2$ and found a good fit with $\chi^2/\mathrm{DF} = 4.6/4$ in the range $x(\Lambda) > 0.2$. The result of the fit is shown as a curve in Fig. 3(b).

C. Backward K_S^0 production

The backward K_S^0's are produced in the target fragmentation region. In the π^+ rest-frame system one considers the deuteron as the projectile and the K_S^0 as the particle produced in the deuteron "projectile" fragmentation region. Hence, the K^0 ($d\bar{s}$) backward production is the result of a recombination of a d quark from the deuteron with a sea antiquark, $\bar{s}$.

The quark-recombination model has been applied to nuclear targets by Berlad, Dar, and Eilam,[9] where they have included the possibility of more than one of the nucleons in the nucleus participating in the interaction. In this model, a hadron-nucleus collision is viewed as a collision with the nucleons lying within a cylinder (tube) of specified cross section along the path of the beam particle through the nucleus. In the case of an interaction with a deuteron nucleus, a tube will contain either exactly one or exactly two nucleons. The distribution of a K_S^0 particle produced from a deuteron target is the sum of the distributions of the K_S^0 produced in a collision with a single nucleon and of the K_S^0 produced in a collision which involves both nucleons in the deuteron, and is given by[9]

$$F(x) = \frac{1}{\pi p^*_{\max}} \int E^* \frac{d^2\sigma}{dx\, dp_T{}^2} = C\sigma_{\mathrm{inel}}^{\mathrm{total}}(d)\left[p_1 \frac{d_p(x) + d_n(x)}{2} + p_2\gamma_2 \frac{\tilde{d}_p(x_d) + \tilde{d}_n(x_d)}{2}\right], \tag{10}$$

where $d_p(x)$ and $d_n(x)$ are the d-quark distributions in the proton and in the neutron as given in Eqs. (9) and (8), respectively. p_1 and p_2 are the probabilities that the interaction occurs with, respectively, one nucleon, or collectively with a tube of two nucleons in the deuteron. p_1 and p_2 can be calculated from Glauber's multiple-scattering theory.[26] Using a Hulthén wave function one gets $p_1 = 0.88$ and $p_2 = 0.12$. γ_2 is an attenuation factor (calculated to be 0.944)[9] which accounts for the possibility that a tube quark may have to penetrate a nucleon in front of it before it can recombine to form a K_S^0.

$\tilde{d}_p(x_d)$ and $\tilde{d}_n(x_d)$ are the distribution functions of the d valence quark in a tube containing two nucleons, evaluated at x_d, the Feynman fractional momentum of the K_S^0 in the overall incident pion and deuteron target ($\pi^+ d$) system. $\sigma_{\mathrm{inel}}^{\mathrm{total}}(d)$ is the total inelastic cross section on deuterium. C is an unknown normalization constant, fixed by fitting the model to the data.

Using the nucleon valence-quark distributions of Eqs. (8) and (9), the valence-quark distributions in the two-nucleon tube are[9]

$$\tilde{d}_p(x) = \int_{y=x}^{1} \left[\frac{315}{256}\frac{(1-y)^4}{\sqrt{y}}\right]\left[12\frac{x}{y}\left(1-\frac{x}{y}\right)\right]\frac{dy}{y} = \frac{63}{16}\left[64x(1+x) + \frac{1-20x-90x^2-20x^3+x^4}{\sqrt{x}}\right] \tag{11}$$

and

$$\tilde{d}_n(x) = \int_{y=x}^{1} \left[\frac{35}{16}\frac{(1-y)^3}{\sqrt{y}}\right]\left[12\frac{x}{y}\left(1-\frac{x}{y}\right)\right]\frac{dy}{y} = 7\left[8x(5+3x) + \frac{1-15x-45x^2-5x^3}{\sqrt{x}}\right]. \tag{12}$$

We have fitted to our data on backward K_S^0 production the predicted form in Eq. (10) using expressions (11) and (12) and have obtained a satisfactory fit with $\chi^2/\mathrm{DF} = 7.3/4$ in the range $x(K_S^0) < -0.2$. The result of the fit is shown as a curve in Fig. 3(a).[27]

D. Backward Λ production

The Λ production in the deuteron fragmentation region could be the result of a recombination of one valence quark (u or d) in the deuteron with a sea diquark (ds or us). The Λ could also be produced by the recombination of a valence diquark (ud) in the deuteron with a sea quark (s).

We first note that for large x the probability of a diquark to carry the large momentum required and to recombine with a single sea quark is much larger than that of a single valence quark to carry a large momentum fraction and recombine with two sea quarks. The valence-diquark

recombination is thus expected to dominate the backward Λ production.

In the first case (recombination of one valence quark in the deuteron with a sea diquark) the x distribution of the Λ will be expressed by Eqs. (10)–(12). The $\cap$ shape of the backward Λ distribution and the clear difference between it and the backward K_S^0 distribution (see Fig. 3) rule out this possibility. This indication was confirmed by the failure to fit Eq. (10) to the data.

In the second case (recombination of a diquark in deuteron with a one sea quark) we expect the x distribution of the produced Λ to be similar to the x distribution of a diquark in the deuteron. From phase-space considerations one gets[28]

$$D(x) = 6x(1-x) \tag{13}$$

for the distribution of a diquark in the nucleon.

Using this expression one may calculate the diquark distribution in a tube of two nucleons (proton and neutron)[9] as follows:

$$\tilde{D}(x) = \int_{y=x}^{1} [6y(1-y)]\left[12\,\frac{x}{y}\left(1-\frac{x}{y}\right)\right]\frac{dy}{y}$$

$$= 72x[2x - 2 - (1+x)\ln x]\,. \tag{14}$$

Then similarly to Eq. (10), one obtains for the x distribution of Λ particles produced by the recombination of a diquark in a nucleon

$$F(x) = C_\Lambda \sigma_{\text{inel}}^{\text{total}}(d)[0.88D(x) + (0.12\times 0.78)\tilde{D}(x_d)]\,. \tag{15}$$

Here we take 0.78 for the attenuation factor γ_2 of a diquark in a deuteron as follows from direct simple calculations.[28]

We have fitted to our data on backward Λ production the functional form in Eq. (15) using expressions (13) and (14) and obtained a good fit with $\chi^2/\mathrm{DF} = 10.3/8$ in the range $x(\Lambda) < -0.2$.[29] The results of the fit are shown as a curve in Fig. 3(b). It is interesting to note that the point at $x(\Lambda) < -1.0$ is kinematically forbidden for an interaction with a nucleon at rest in the deuteron. However, the point is allowed by Fermi motion in the deuteron or by a collective interaction involving more than one nucleon in the target. Such points are theoretically expected[9] and experimentally found in other experiments.[30]

VII. SUMMARY AND CONCLUSIONS

We have measured the inclusive cross section for K_S^0, Λ, and $\bar{\Lambda}$ production in $\pi^+ d$ interaction at 24 GeV/c and obtained

$$\sigma(K_S^0) = (2.50 \pm 0.13)\ \text{mb},$$

$$\sigma(\Lambda) = (1.62 \pm 0.09)\ \text{mb},$$

$$\sigma(\bar{\Lambda}) = (0.12 \pm 0.02)\ \text{mb}.$$

The topological cross sections all peak at four prongs.

The average charge multiplicities are $\langle n_{\text{ch}}\rangle = 4.93 \pm 0.04$, 4.95 ± 0.05, and 4.69 ± 0.18 for K_S^0, Λ, and $\bar{\Lambda}$ production, respectively. About 65% of the K_S^0 and the $\bar{\Lambda}$ events are produced in the forward hemisphere of the center-of-mass system, while 78% of the Λ events are produced in the backward hemisphere.

The invariant cross sections

$$F(x) = \frac{1}{\pi p_{\text{max}}^*}\int E^* \frac{d^2\sigma}{dx\,dp_T{}^2}\,dp_T{}^2$$

for K_S^0 and for Λ production peak at $x \cong 0.1$ and at $x \cong -0.5$, respectively, as observed in other experiments at nearby and at Fermilab energies as well.[1-5] The transverse-momentum-squared distributions $d\sigma/dp_T{}^2$ behave for small $p_T{}^2$ like $ae^{-bp_T{}^2}$ with $b(K_S^0) = 4.3 \pm 0.1$, $b(\Lambda) = 3.14 \pm 0.09$, and $b(\bar{\Lambda}) = 2.7 \pm 0.48$ $(\text{GeV}/c)^{-2}$. For K_S^0 production there is a break in the slope b at $p_T{}^2 \cong 0.6$ $(\text{GeV}/c)^2$ after which it becomes equal (within errors) to $b(\Lambda)$.

The invariant cross section

$$F(x, p_T{}^2) = \frac{E^*}{\pi p_{\text{max}}^*}\,\frac{d^2\sigma}{dx\,dp_T{}^2}$$

does not seem to factorize with respect to x and $p_T{}^2$.

The average charge multiplicity $\langle n_X\rangle$ of the system of particles produced with the Λ is consistently higher for any value of the system mass M_X than the corresponding $\langle n_X\rangle$ for the K_S^0. For both K_S^0 with $\cos\theta^* > 0.5$ and Λ with $\cos\theta^* < -0.5$, $\langle n_X\rangle$ behaves like $A + B\ln M_X{}^2$, with $B(K_S^0) = 2.2 \pm 0.26$ and $B(\Lambda) = 1.2 \pm 0.25$.

The polarization of the Λ is not zero, and it has a structure as a function of x. In the high-p_T region, the magnitude of the polarization increases with p_T (note that the polarization is negative with the sign convention which we have adopted).

The average polarization of the Λ's for $x(\Lambda) < -0.2$ is $p = -0.10 \pm 0.03$. The x distributions for K_S^0 and Λ production are well described by the quark-recombination model. The forward K_S^0 and Λ invariant cross sections $F(x)$ are satisfactorily described by the form $A(1-x)^2$, consistent with a predicted x distribution of a valence quark inside the π^+ projectile which recombines with sea quarks to form K_S^0 or Λ particles in the beam fragmentation region.

The backward K_S^0 invariant cross section $F(x)$ resembles the distribution functions of a quark inside a nucleon [Eqs. (8) and (9)], consistent with

a mechanism according to which the backward K_S^0 is produced in the target fragmentation region by recombination of a quark in the deuteron with a sea quark.

The backward Λ production, as theoretically expected, is well described by the recombination of a diquark inside the deuteron with a sea quark, rather than recombination of one quark inside the deuteron with two sea quarks.

ACKNOWLEDGMENT

We thank our scanning and measuring staffs for their contribution. We express our gratitude to A. Dar and G. Berlad for their contribution to the interpretation of the data. We would like to extend our thanks to the Johns Hopkins University high-energy group and in particular to Professor A. Pevsner for making the film available to us.

[1]P. Bosetti *et al.*, Nucl. Phys. B94, 21 (1975).
[2]P. H. Stuntebeck *et al.*, Phys. Rev. D 9, 608 (1974).
[3]F. Barreiro *et al.*, Phys. Rev. D 17, 669 (1978).
[4]D. Brick *et al.*, Nucl. Phys. Bi64, 1 (1980).
[5]H. Kichimi *et al.*, Phys. Rev. D 20, 37 (1979).
[6]G. Charlton *et al.*, Phys. Rev. Lett. 30, 574 (1973).
[7]D. Ljung *et al.*, Phys. Rev. D 15, 3163 (1977).
[8]D. Bogert *et al.*, Phys. Rev. D 16, 2098 (1977).
[9]G. Berlad, A. Dar, and G. Eilam, Phys. Rev. D 22, 1547 (1980).
[10]P. Schmid, in *Proceedings of the XVIII International Conference on High Energy Physics, Tbilisi, 1976,* edited by N. N. Bogolubov *et al.* (JINR, Dubna, 1977), Vol. I, p. A2-9.
[11]W. R. Frazer and D. R. Snider, Phys. Lett. 45B, 136 (1973); C. F. Chan, Phys. Rev. D 8, 179 (1973).
[12]Particle Data Group, Phys. Lett. 75B, 1 (1978).
[13]S. L. Meyer, *Data Analysis for Scientists and Engineers* (Wiley, New York, 1975), p. 332.
[14]S. Erhan *et al.*, Phys. Lett. 82B, 301 (1979).
[15]W. Ochs, Nucl. Phys. B118, 397 (1977).
[16]G. Miller *et al.*, Phys. Rev. D 5, 528 (1972).
[17]A. Bodek *et al.*, Phys. Rev. Lett. 30, 1087 (1973).
[18]K. P. Das and R. Hwa, Phys. Lett. 68B, 459 (1977).
[19]L. Van Hove, CERN Report No. TH2580, 1978 (unpublished).
[20]R. D. Field and R. P Feynman, Phys. Rev. D 15, 2590 (1977).
[21]Z. F. Ezawa, Nuovo Cimento 23A, 271 (1974).
[22]E. I. Berger and S. J. Brodsky, Phys. Rev. Lett. 42, 940 (1979).
[23]Chicago-Princeton Collaboration, K. J. Anderson *et al.*, Report No. EFI 79-34, 1979 (unpublished).
[24]The distribution $(1-x)^1$ does not match our K° data. When left free in the fit, the power is found to be 1.79 ± 0.21 with $\chi^2/\mathrm{ND} = 10.1/6$ for $x > 0.2$, compatible with 2. This result does not depend on the lower cut up to $x_{\mathrm{cut}} = 0.6$.
[25]Here the power of $(1-x)$ is found to be 1.55 ± 0.42 with $\chi^2/\mathrm{ND} = 3.74/3$ for $x > 0.2$, compatible with the result obtained for the K° sample. However, there is not enough statistics to study the dependence upon the cutoff.
[26]R. J. Glauber, in *High Energy Physics and Nuclear Structure,* edited by G. Alexander (North-Holland, Amsterdam, The Netherlands, 1967), p. 311.
[27]The single free parameter in this fit is C, found to be 38.6 ± 3.4.
[28]G. Berlad, S. Dado, and A. Dar (unpublished).
[29]The single free parameter in this fit is C_Λ, found to be $C_\Lambda = 177.7 \pm 7.0$.
[30]See for example, A. M. Baldin, Fiz. Elem. Chastits At. Yadra 8, 429 (1977) [Sov. J. Part. Nucl. 8, 175 (1977)]; J. Papp *et al.*, Phys. Rev. Lett. 34, 601 (1975).